Since January 2020 Elsevier has created a COVID-19 resource centre with free information in English and Mandarin on the novel coronavirus COVID-19. The COVID-19 resource centre is hosted on Elsevier Connect, the company's public news and information website.

suggesting irradiation dose-responsiveness, which was correlated with interstitial and intracellular edema. CD68 immunostaining accompanying vacuolization suggested mononuclear cell infiltration. These changes were prominent in working myocardium but not cardiac conduction tissue. Intracardiac conduction represented by PR and QTc intervals on ECG was delayed compared to baseline measurements. ST segment was initially depressed and gradually elevated. Ventricular chamber dimensions and function remained intact without pericardial effusion.

Conclusion

Mononuclear cell-related intra- and extracellular edema with diffuse vacuolization and intercalated disc widening were observed within 1 month after high-dose irradiation. ECG indicated intracardiac conduction delay with prominent ST-segment changes. These observations suggest that early antiarrhythmic effects after cardiac radioablation result from conduction disturbances and membrane potential alterations without necrosis.

PO-1915 Macrophages subpopulations in stereotactic radiation-induced lung injury in mice.

S. Braga-Cohen[1], M. Dos Santos[2], J. Baijer[3], F. Milliat[1], A. Françoi[1]

[1]Institute for radiation protection and nuclear safety, Health division LRMed, Fontenay-aux-Roses, France; [2]Institute for radiation protection and nuclear safety, Health division LRacc, Fontenay-aux-Roses, France; [3]French Atomic energy commission , IRCM, Fontenay-aux-Roses, France

Purpose or Objective

Stereotactic radiotherapy is a therapeutic alternative for 20-30% of patients with localised primary bronchial cancer and considered at high surgical risk. It is a high ballistic precision technique using small converging beams irradiating very small volumes at high doses. Despite accurate targeting, some patients develop inflammatory or fibrotic pneumopathies. The laboratory has developed a model of stereotactic pulmonary irradiation in mice showing an important macrophage infiltrate within the focal lesion. Macrophages are immune cells known to be involved in radiation-induced fibrotic processes. They are polarised cells that evolve in a functional continuum from M1, pro-inflammatory, to M2, anti-inflammatory. The aim of this project is to determine the role of macrophage sub-populations in the development of lung damage induced by irradiation under stereotactic conditions in mice. This may open up new therapeutic perspectives in the management of the pulmonary sequelae of SBRT.

Materials and Methods

Mouse left lung was irradiated with the SARRP (Small Animal Radiation Research Platform) using a 3 x 3 mm^2 collimated beam delivering arc-therapy over 220 degrees. We compared 60 and 80 Gy single doses, inducing progressive and rapid fibrosis, respectively. Experiments were performed from 3 days to 12 months post-irradiation. Immunohistology allowed macrophages subtypes localization within focal lesions all along the observation period. Flow cytometry provided informations on the distribution of these subpopulations in the pulmonary parenchyma and broncho-alveolar space. Finally, lung lesions in wild type mice (WT) and CCR2 deficient mice (CCR2KO) in which macrophage recruitment is abrogated, were compared, in order to understand the influence of macrophage recruitment in the severity of lung radiation damage.

Results

In WT mice, lung fibrosis developed 3 months post-80 Gy and 6 months post-60 Gy exposure. Studies at earlier time points are in progress. Immunohistology revealed mainly M2 type macrophage infiltration after both irradiation doses. The kinetics and the aspect of the patch are similar between WT and CCR2KO mice following 80 Gy. In contrast, after 60 Gy, injury patch appeared less severe in CCR2KO mice compared to WT mice. Immunohistological studies are in progress to confirm these first observations. A panel of 12 markers has been created and validated for flow cytometry studies, allowing the precise characterisation of the macrophagic sub-populations invading damaged lung. These analyses could reveal different macrophage populations in both strains of mice which could be decisive in explaining differencies in lung damage severity.

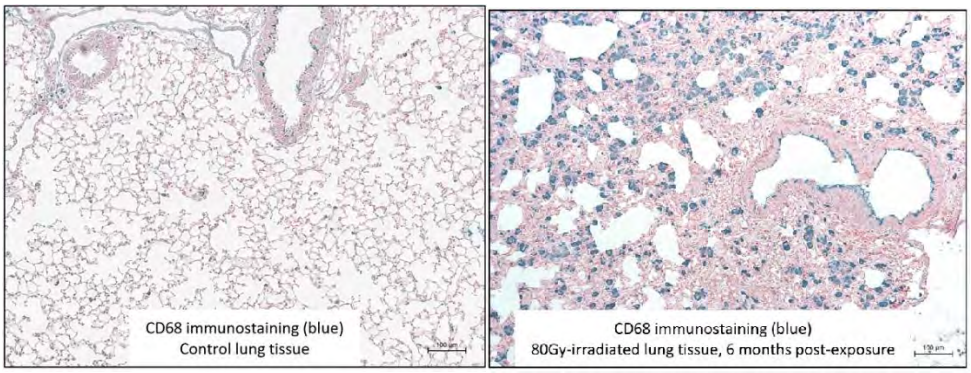

Conclusion

In conclusion, many analyses remain to be done but the first results seem to support a role for some macrophage populations in the development of focal lung lesions. The project will continue by using parabiosis experiments in order to determine if there is a circulating origin of some macrophage subpopulations invading lung tissue.

PO-1916 Low-dose lung radiotherapy for COVID-19 pneumonia: preclinical studies in bleomycin pneumonitis

A. Chalmers[1], M. Jackson[1], K. Stevenson[1], S. Chahal[1], E. Curley[1], G. Finney[2], R. Gutierrez-Quintana[3], E. Onwubiko[4], A. Rupp[3], K. Strathdee[1], M. MacLeod[2], C. McSharry[2]

[1]University of Glasgow, Institute of Cancer Sciences, Glasgow, United Kingdom; [2]University of Glasgow, Institute of Infection, Immunity and Inflammation, Glasgow, United Kingdom; [3]University of Glasgow, School of Veterinary Medicine, Glasgow, United Kingdom; [4]University of Glasgow, Cancer Research UK Beatson Institute , Glasgow, United Kingdom

Purpose or Objective

Low-dose whole lung radiotherapy (LDLR) has been proposed as a treatment for patients with acute respiratory distress

syndrome associated with SARS-CoV-2 infection and clinical trials are underway. There is an urgent need for preclinical evidence to justify this approach and inform dose, scheduling, patient selection and mechanisms of action. To address this need, we undertook preclinical studies using a mouse model of bleomycin induced pneumonitis, which reproduces many of the pathophysiological changes of COVID-19 lung disease including epithelial cytopathy, endotheliitis, inflammatory infiltrates and surfactant loss.

Materials and Methods

Female C57BL/6 mice were treated with intranasal bleomycin sulphate (7.5 or 11.25 units/kg, day 0), then exposed to whole lung radiation therapy (0.5, 1.0, 1.5 Gy or sham, day 3). Bodyweight was measured daily and lung tissue harvested for histology (left lung) and flow cytometry (right lung) on day 10. Computed tomography (CT) lung imaging was performed pre-radiation (day 3) and pre-endpoint (day 10).

Results

Bleomycin caused pneumonitis of variable severity which correlated with weight loss (p=0.005). LDLR at 1.0 Gy was associated with a significant increase in the proportion of mice recovering to 98% of initial bodyweight by day 10 (21.2% v. 3.3% in sham irradiated controls, p=0.03; Fig 1) and a proportion of these mice exhibited less severe histopathological lung changes at day 10. Mice experiencing moderate initial weight loss were significantly more likely to respond to LDLR than those experiencing severe initial weight loss (p<0.01). Additionally, LDLR (1.0 Gy) significantly reduced bleomycin-induced increases in interstitial macrophages (p<0.01), CD103+ dendritic cells (p<0.001) and neutrophil-DC hybrids (p<0.05) but did not modulate the bleomycin associated reduction in alveolar macrophages (Fig 2). Consistent with previous reports describing more marked effects of inhaled bleomycin in the left lungs, bleomycin-treated mice exhibited significantly lower percentages of aerated lung in left than right lungs at day 3 (53% v 70%, p<0.001); LDLR (1.0 Gy) prevented further reductions in aerated lung volume in right but not left lungs (p<0.05). LDLR at 0.5 and 1.5 Gy did not modulate bodyweight or flow cytometric readouts of bleomycin-induced pneumonitis.

Figure 1

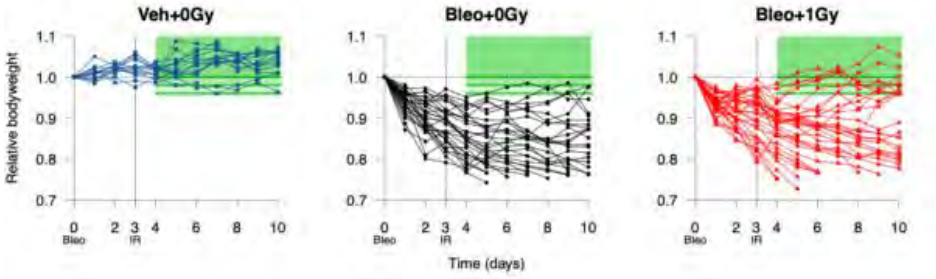

Figure 2

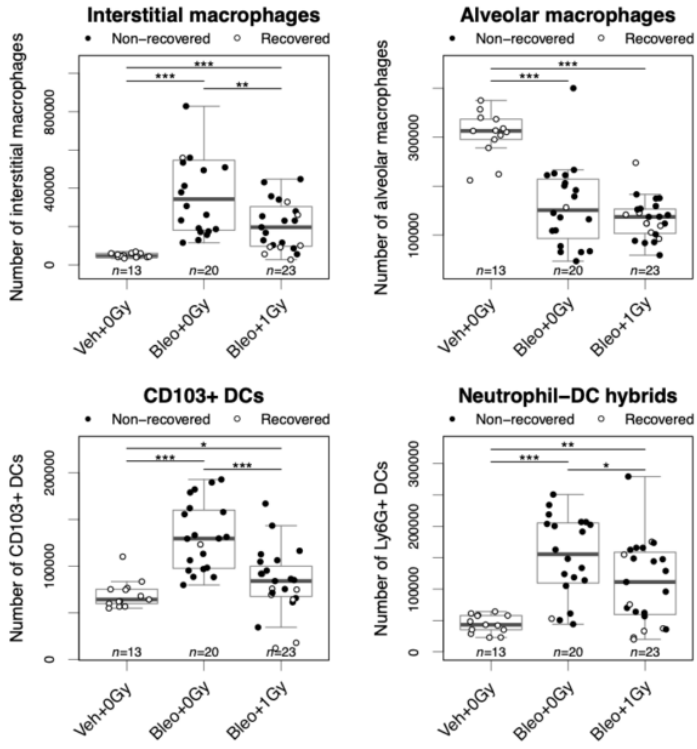

Conclusion

Our data support the concept that LDLR can ameliorate acute inflammatory lung injury, identify 1.0 Gy as the most

effective dose and provide evidence that it is more effective in the context of moderate than severe pneumonitis. Mechanistically, LDLR at 1.0 Gy significantly suppressed bleomycin-induced accumulation of pulmonary interstitial macrophages, CD103+ dendritic cells and neutrophil-DC hybrids.

PO-1917 Circadian rhythm effects on radiotherapy toxicity

C. Talbot[1], A. Webb[1], E. Harper[1], D. Azria[2], A. Choudhury[3], D. De Ruysscher[4], A. Dunning[5], R. Elliott[3], S. Kerns[6], M. Lambrecht[7], T. Rancati[8], B. Rosenstein[9], P. Seibold[10], E. Sperk[11], A. Vega[12], L. Veldeman[13], J. Chang-Claude[14], C. West[3], T. Rattay[15], R.P. Symonds[16]

[1]University of Leicester, Genetics, Leicester, United Kingdom; [2]Montpellier Cancer Institute, Department of Radiation Oncology, Montpellier, France; [3]University of Manchester, Division of Cancer Sciences, Manchester, United Kingdom; [4]Maastricht University Medical Center, Department of Radiation Oncology (Maastro clinic), Maastricht, The Netherlands; [5]University of Cambridge, Centre for Cancer Genetic Epidemiology, Cambridge, United Kingdom; [6]University of Rochester, Department of Radiation Oncology , Rochester, NY, USA; [7]UZ Leuven, Radiation Oncology, Leuven, Belgium; [8]Fondazione IRCCS Istituto Nazionale dei Tumori, Prostate Cancer Program, Milano, Italy; [9]Icahn School of Medicine at Mount Sinai, Department of Radiation Oncology, New York, USA; [10]German Cancer Research Center (DKFZ), Division of Cancer Epidemiology, Heidelberg, Germany; [11]Medical Faculty Mannheim, Department of Radiation Oncology, Mannheim, Germany; [12]Fundación Pública Galega Medicina Xenómica, Instituto de Investigación Sanitaria, Santiago de Compostela, Spain; [13]Ghent University Hospital, Department of Radiation Oncology, Ghent, Belgium; [14]University Medical Center Hamburg-Eppendorf, University Cancer Center , Hamburg, Germany; [15]University of Leicester, Leicester Cancer Research Centre, Leicester, United Kingdom; [16]University of Leicester, Leicester Canceer Research Cenre, Leicester, United Kingdom

Purpose or Objective

To test whether there is evidence for a genetically modified time-of-day effect on toxicity after radiotherapy for breast cancer

Materials and Methods

We collected time of each radiotherapy fraction from patients in the LeND and REQUITE breast cancer cohorts. LeND is a UK retrospective cohort collected 2008-10 with 661 patients. Requite was a multi-centre, prospective study in Europe and US (www.requite.eu). Enrolment was open for two and a half years through 26 centres in eight countries. Follow-up was collected for 2.5 years ending in September 2018. The primary endpoints used were acute erythema and late breast atrophy assessed by CTCAE v4. 4438 patients were enrolled in REQUITE, of which 2069 breast cancer patients.

Results

We earlier showed that genetic variation in the *NOCT* and *PER3* genes predisposed some patients to have worse overall late toxicity if irradiated in the morning compared with afternoon, with less clear results on acute toxicity. In a new study we have carried out a more sophisticated time analysis on a larger cohort.

For the acute toxicity end-point of erythema we find an association with the *PER3* gene but not time-of-day. For late toxicity, multivariate analysis shows a peak for atrophy in the afternoon with the effect reversed for variants of the *PER3* and *CLOCK* genes.

Conclusion

In summary we report results that refine our understanding of time-of-day effects on radiotherapy and suggest that target tissues may have different peak times for toxicity dependant on genotypes within known circadian genes.

PO-1918 Studying radioinduced damage to microvasculature through 3D in-vitro models

T. Rancati[1], L. Possenti[1], L. Mecchi[2], A. Cicchetti[1], C. Arrigoni[3], D. Petta[4], S. Bersini[4], R. El Bezawy[5], V. Doldi[5], T. Giandini[6], C. Stucchi[6], M.L. Costantino[7], M. Moretti[4]

[1]Fondazione IRCCS Istituto Nazionale dei Tumori, Prostate Cancer Program, Milan, Italy; [2]Ente Ospedaliero Cantonale, Regenerative Medicine Technologies Laboratory, Servizio di Ortopedia e Traumatologia,, Lugano, Switzerland; [3]Ente Ospedaliero Cantonale, Regenerative Medicine Technologies Laboratory, Servizio di Ortopedia e Traumatologia, Lugano, Switzerland; [4]Regenerative Medicine Technologies Laboratory, Servizio di Ortopedia e Traumatologia, Ente Ospedaliero Cantonale, Lugano, Switzerland; [5]Fondazione IRCCS Istituto Nazionale dei Tumori, Molecular Pharmacology, Milan, Italy; [6]Fondazione IRCCS Istituto Nazionale dei Tumori, Medical Physics, Milan, Italy; [7]Politecnico di Milano, Department of Chemistry, Materials and Chemical Engineering "Giulio Natta", , Milan, Italy

Purpose or Objective

Present first results on use of 3D in-vitro models to study radioinduced damage to microvasculature

Materials and Methods

Microfluidic chips (Fig.1a) were produced in polydimethylsiloxane (PDMS) via soft lithography and then stitched to a coverslip glass, following the procedure proposed by Chen (Nat Prot 2017). PDMS chip is obtained using a 3D printed mold, allowing the creation of a specifically designed geometry. The chip is constituted by 3 parallel channels; such a configuration enables the confinement of a mixture of cells and a gel in the central channel. Leveraging on this feature, a microvascular network is seeded and cultured on the chip.

We seeded Human Umbilical Vein Endothelial Cells (HUVEC) at 6.25M/ml, using as a supporting gel a fibrin-thrombin gel (fibrinogen at 5mg/ml, thrombin at 4U/ml). The culture media is inserted in the lateral channels after the seeding and replaced daily. On day4, a monolayer of HUVEC is seeded in the lateral channel at the concentration of 1.5M/ml following the method proposed by Offeddu (Small 2019). Microvascular network is cultured till day8.

We run perfusion tests on day7, inserting a fluorescent solute (Dextran, TRITC) in the lateral channels (Fig.1d). The image shows a perfused network, as the fluorescent dye has filled the network and not the gel outside the network (seen as black).

On day8, chips were irradiated (6MeV LINAC-1.4Gy/min, Fig.1b) with different doses/fractionation (Fig.2a). An irradiation (IR) phantom (Fig.1c) was used to ensure accurate dose computation (electronic equilibrium at sample depth).

The samples were fixed with PFA 2-3-24h after IR. DNA damage was evaluated by g-H2AX and apoptosis by caspase3. Both analyses were conducted by immunofluorescence. The samples were imaged by a confocal microscope (Fig.1e-1f). Data were quantified in terms of area positive to damage with respect to nuclei area (defined as "Apoptotic" or "Damaged Fractions")